

University of Arkansas, Fayetteville

ScholarWorks@UARK

---

Electrical Engineering Undergraduate Honors  
Theses

Electrical Engineering

---

5-2009

## Preliminary study based on the DDSCAT software to explore increasing the contrast of breast tumors for microwave imaging

Rachel Megee

*University of Arkansas, Fayetteville*

Follow this and additional works at: <https://scholarworks.uark.edu/eleguht>



Part of the [Biomedical Commons](#), and the [Systems and Communications Commons](#)

---

### Citation

Megee, R. (2009). Preliminary study based on the DDSCAT software to explore increasing the contrast of breast tumors for microwave imaging. *Electrical Engineering Undergraduate Honors Theses* Retrieved from <https://scholarworks.uark.edu/eleguht/8>

This Thesis is brought to you for free and open access by the Electrical Engineering at ScholarWorks@UARK. It has been accepted for inclusion in Electrical Engineering Undergraduate Honors Theses by an authorized administrator of ScholarWorks@UARK. For more information, please contact [scholar@uark.edu](mailto:scholar@uark.edu).



**PRELIMINARY STUDY BASED ON THE DDSCAT SOFTWARE TO EXPLORE  
INCREASEING THE CONTRAST OF BREAST TUMORS FOR MICROWAVE  
IMAGING**

PRELIMINARY STUDY BASED ON THE DDSCAT SOFTWARE TO EXPLORE  
INCREASEING THE CONTRAST OF BREAST TUMORS FOR MICROWAVE  
IMAGING

A thesis submitted to the Honors College in partial  
fulfillment of the requirements for the degree of  
Honors Bachelor of Science  
in Electrical Engineering

By

Rachel Lauren Megee

May 2009  
University of Arkansas

## **ABSTRACT**


Microwave technology is being researched for its capabilities to detect breast tumors less painfully and at earlier stages. It is necessary to have a large contrast between cancerous and healthy tissue when the microwaves are reflected off the breast tissue. To model the increasing contrast between cancerous breast tissue and healthy breast tissue, the DDSCAT code is investigated for its capabilities and analyzed for its accuracy in scattering calculations.

The DDSCAT is used to model homogenous and inhomogeneous targets. Simulations of the scattering field by the homogeneous and inhomogeneous targets are conducted and compared to Mie theory calculations for accuracy. Many different magnitudes of refractive indices, as well as real and complex refractive indices, are tested with the DDSCAT.

Overall, the results obtained, show the DDSCAT to be a flexible code, capable of modeling many complex targets, which offers a potential to further research of breast cancer detection.

This thesis is approved for recommendation to the Graduate Council.

Thesis Director:



Dr. Magda El-Shenawee

**THESIS DUPLICATION RELEASE**

I hereby authorize the University of Arkansas Libraries to duplicate this thesis when needed for research and/or scholarship.

Agreed 

Refused \_\_\_\_\_

## **ACKNOWLEDGEMENTS**

I thank Dr. El-Shenawee, my thesis advisor, for all of her encouragement, support, and the wonderful opportunity she gave me to research abroad in France. She is very devoted to her students and always made time to meet with me to answer my questions regarding my research project. She encouraged me to work hard, constantly learn, and to pursue higher learning in graduate school. Her encouragement allowed me to challenge myself and reach higher to achieve success in my research and academic career here at the University of Arkansas.

I also thank my mother and father who have constantly pushed me to be successful academically. They have continually supported me in my academic endeavors and given me the wisest counsel about all areas of life. I am extremely grateful for their continual investment in my life.



## TABLE OF CONTENTS

### 1. Introduction

1.1 Problem: Breast Cancer.....	1
1.2 Thesis Statement.....	2
1.3 Approach.....	3
1.4 Potential Impact.....	3
1.5 Organization of Thesis.....	4

### 2. Background

2.1 Contrast of Breast Tissues.....	5
2.2 Introduction to DDSCAT.....	5
2.2.1 Executable Files and Output Files.....	8
2.2.2 Solvers and Simulation.....	9
2.3 Mie Theory.....	10

### 3. Approach and Implementation

3.1 Iterative Solver Simulations.....	11
3.2 Homogeneous Target Simulations.....	13
3.3 Inhomogeneous Target Simulations.....	15

### 4. Analysis

4.1 Analysis of Iterative Solvers.....	19
4.2 Analysis of the Homogeneous Target Simulations.....	20
4.3 Analysis of the Inhomogeneous Target Simulations.....	21

### 5. Conclusion

5.1 Summary.....	23
------------------	----

### References

## LIST OF FIGURES

Figure 1 Lab Frame.....	7
Figure 2 Fractional Error vs. Iterations for PBCGST solver.....	12
Figure 3 Fractional Error vs. Iterations for PETRKP.....	13
Figure 4 Spherical Homogeneous Target with $m=6.0$ using 8, 19, 32, and 81 Dipoles .....	14
Figure 5 Homogeneous spherical Target with $m=6+0.01j$ using 2197 Dipoles .....	15
Figure 6 Geometry for scattering of an Inhomogeneous Target [x].....	16
Figure 7 Efficiencies of Scattering for a Coated Sphere for $\nu=1.6$ .....	17
Figure 8 Efficiencies for Scattering with $q=0.2$ .....	18

# 1. INTRODUCTION

## 1.1 Problem: Breast Cancer

Breast cancer is the leading cause of death from cancers among women in the United State except for lung cancer [1]. In 2008 there were 182,460 diagnoses of breast cancer in women and 40,480 deaths in the United States [2]. Breast cancer, however, affects women all over the world. Around 1.3 million women around the world are diagnosed annually with breast cancer and over 465,000 women do not survive this cancer [1].

Breast cancer can affect women of all ages, but it is usually more prevalent in older women. By the age of sixty, one in twenty-six women have a chance of developing breast cancer [1]. This is a large probability compared to one out of two hundred twenty-nine women develop breast cancer by age thirty [1]. Although older women are at high risk for breast cancer, the survival rate of women sixty and older is much higher than for women in their thirties [1]. Surviving breast cancer is also dependent of the stage of the cancer when it is detected. Stage I breast cancer has a 100% survival rate over a five year period [1]. However, Stage IIIB only has a 54% survival rate and Stage IV a 20% survival rate over a five year period [1].

Because of these daunting statistics, it is necessary to detect breast cancer in its early stages. Detecting breast tumors can be difficult because the tumors usually begin to develop in the ducts of the breast. Currently, the mammogram, MRI, CAT scan, and ultrasound are used to detect breast tumors with the mammogram being the most common detection method.

The mammogram uses x-rays to create an image of the breast on high contrast and high resolution film. Even though the mammogram can detect up to 85% of breast cancers, it contains some drawbacks [1]. First of all, a breast tumor is not visible if the cancer is small [1]. Also, a breast tumor will not show up on the mammogram film if it is hidden under the arm or in a hard to image area [1]. Finally, other shadows can hide breast tumors making them hard to detect [1]. Another drawback to the mammogram is the pain a woman endures during the clinical screening. During a mammogram, the breast is compressed and flattened on to the film. X-rays are applied to the film and it is exposed to image the breast [2]. This process of flattening the breast tissue causes tremendous pain resulting in women not requesting their routine mammograms.

It is for these reasons that Dr. El-Shenawee is conducting research to form a new method of breast cancer detection. Her research focuses on using microwaves to penetrate breast tissue and capturing the reflection of the microwaves with antennas, The data received by the antennas is then transmitted to a computer where it can be processed to image the breast and breast tumors. In this case, it is highly important that the reflection of the microwaves from the healthy breast tissue as compared to a breast tumor have significant contrasts. The extent of this thesis seeks to validate a program capable of analyzing the increased contrast of microwave reflections off of materials with different refractive indices.

## **1.2 Thesis Statement**

It is the goal of this research to verify the accuracy of the DDSCAT as a modeling tool by comparing it to theoretical calculations conducted with Mie Theory. The

DDSCAT simulations will be used to show the contrast between healthy and unhealthy breast tissue when microwaves are applied.

### **1.3 Approach**

To simulate the contrast between healthy breast tissue and unhealthy tissue, a target, model of the breast, is constructed. The DDSCAT is capable of composing various targets as specified. Homogeneous targets and inhomogeneous targets with differing refractive indices are constructed and the scattering magnitudes of a microwave field are simulated.

The spherical homogeneous targets are composed of varying numbers of dipoles and radii. The targets are tested with real and complex refractive indices, incident and orthogonal polarizations, and multiple orientations. The results of the simulations are compared to Mie Theory graphs with the same refractive indices as the target. The same method is used to simulate the spherical inhomogeneous targets.

All of the simulations are conducted in FORTRAN 95 programming language. The accuracy of the DDSCAT simulations for homogeneous and inhomogeneous targets is evaluated as well as the iterative solver algorithms and the CPU time taken to complete simulations for each target.

### **1.4 Potential Impact**

With the success of gathering an enhanced microwave reflection from spherical particles using the DDSCAT to model the reflection, extensive research can be performed to implement complex shapes. By utilizing the complex shapes the code offers, these

shapes can be used to more accurately represent a breast tumor. The code also offers extended capabilities to create any target shape the user would like to define. Having this flexibility in a code and a code that is accurate and computes quickly will have a great positive effect on the overall modeling of the contrast of breast tissues in a microwave field.

### **1.5 Organization of Thesis**

This thesis is organized into five chapters. The introduction chapter gives insight into the problem, defines the thesis statement, and address the approach to research and the potential impact. The background section covers the need to model an increased contrast in breast tissues, the operation of the DDSCAT code used for simulations, and the theory the DDSCAT simulations are compared to for accuracy. The third chapter gives a description of the research approaches that are performed. The fourth chapter discusses the results of the research and the fifth chapter addresses the conclusions drawn.

## **2. BACKGROUND**

### **2.1 Contrast of Breast Tissues**

Past research in breast tumor detection using microwaves has shown a contrast between healthy breast tissue and cancerous breast tissue when microwaves are applied. However, recent studies, performed on women of all ages, have shown a poor contrast with healthy and unhealthy tissue, making a tumor difficult to detect. The Department of Electrical Engineering at the U of A is currently conducting research that mixes biology and microwaves in the area of breast tumor detection. The current NSF research award no. ECS-0524042 of Dr. El-Shenawee focuses on developing a new method of detecting breast tumors using microwave-imaging techniques. Unlike the mammogram, this approach proposes a non-invasive, non-ionizing method to attain more accurate results and earlier detection. To improve the contrast of a breast tumor with surrounding healthy tissue, a method using gold nanoparticles has been proposed. The gold nanoparticles can be functionalized biochemically to “stick” to cancerous tissue. It is expected that this contrast enhancement will facilitate the microwave imaging process of the tumor, from the scattering information generated from its interaction with an incident field. This technique is being researched using the DDSCAT program.

### **2.2 Introduction to the DDSCAT**

Different rigorous and approximation methods have been proposed to study the interaction between electromagnetic fields and matter. However, incorporating the modeling capabilities of the DDSCAT into the overall research project is investigated. Although the operational principles of the DDSCAT are published elsewhere, it is

convenient to briefly describe them. The DDSCAT code developed at Princeton University is free software based on the discrete dipole approximation (DDA). The software was developed by Drain and Flatau [4] and is “a very flexible and general technique for calculating the optical properties of particles of arbitrary shapes. The DDA replaces the solid particle by an array of  $N$  point dipoles, with the spacing between the dipoles small compared to the wavelength. Each dipole has an oscillating polarization in response to both an incident plane wave and the electric fields due to all of the other dipoles in the array; the self-consistent solution for the dipole polarizations can be obtained as the solution to a set of coupled linear equations.” [4] The targets are generated in general by the following equations where the relation to the volume of the target, affective radius, and number of dipoles can be seen.

$$V = Nd^3 \tag{2.1}$$

$$a_{eff} \equiv \left(\frac{3V}{4\pi}\right)^{\frac{1}{3}} \tag{2.2}$$

Various target geometries, generated by the dipole arrays, can be represented [3]. A representation of a spherical target modeled with dipoles can be seen in Figure 1 of reference [4].

Once the target geometry has been selected, it is necessary to represent the volume with an adequate number of dipoles, in which  $d$  is the separation between two dipoles, A function of the surface irregularity  $f(N)$ , is used to find minimum points of  $N$  dipoles [4]. The computing time of the software is related to the square of the number of dipoles [4]. By locating the minimum points of the function  $f(N)$ , an adequate number of



dipoles can be obtained to compose the target geometry without sacrificing CPU time.

The equation below shows  $f(N)$ .

$$f(N) \equiv \left(\frac{5}{3}\right) \left(\frac{4\pi}{3}\right)^{\frac{2}{3}} N^{\frac{-5}{3}} \sum_{i=1}^N \left(x_i^2 + y_i^2 + z_i^2 + \frac{d^2}{12}\right) \quad (2.3)$$

Along with target geometry and selecting an adequate amount of diopoles, polarization and orientation of the target must be set up. The ‘‘Lab Frame’’ for the target is shown below. This illustrates the direction of incident polarization on the target along the x-axis and the position and orientation setup of the target geometry.

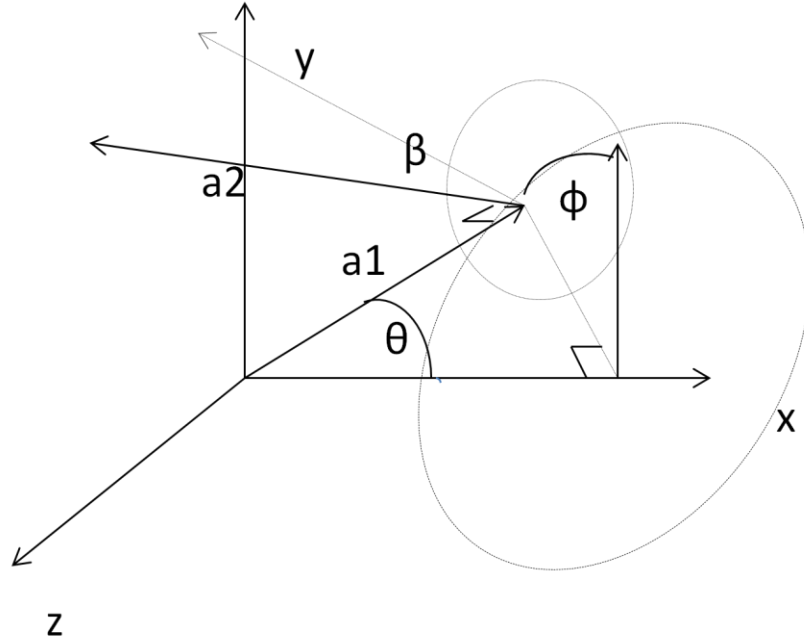


Figure 1. Lab Frame

The input file allows the polarization to be set to IORTH=1 for incident polarization and IORTH=2 for both incident and orthogonal polarization [3]. Once the user specifies the first polarization state  $\vec{e}_{i1}$ , the DDSCAT calculates the corresponding polarization by  $\vec{e}_{i\parallel} = \vec{x} \times \vec{e}_{i\perp}$  which is orthogonal to the first state [3]. The polarization

states are related to the other axis using Eq. 2.4. The Stoke's Parameters and the Mueller Matrix calculate the desired polization within a DDCSCAT subroutine [3].

$$\begin{pmatrix} \hat{y} \\ \hat{z} \end{pmatrix} = \begin{pmatrix} \cos \phi_s & \sin \phi_s \\ \sin \phi_s & -\cos \phi_s \end{pmatrix} \begin{pmatrix} \hat{e}_{i||} \\ \hat{e}_{i\perp} \end{pmatrix} \quad (2.4)$$

If the spherical target is not a continuum target, the polarization of the dipoles changes at the corners, in which  $\phi_s$  is the scattering azimuth angle [4]. According to reference [4] this could lead to error in calculations of spherical targets depending on the size of the target and the magnitude of the refractive index.

The target must be setup in the Lab Frame (LF) in case rotation and further orientation of the target is required during simulation. The target must be orientated according to the incident polarization axis and this can be done with two methods [3].

1. specifying the direction of  $\mathbf{a1}$  and  $\mathbf{a2}$  in the LF, or
2. specifying the directions of  $\mathbf{x}$  (incidence direction) and  $\mathbf{y}$  in the Target Frame.

These methods are accomplished by specifying the values of variables  $\beta$ ,  $\Phi$ ,  $\Theta$  in the input file, ddscat.par. This executable file is explained in the following section.

### 2.2.1 Executable Files and Output Files

The DDSCAT contains two executables, ddscat and CALLTARGET, which can be manipulated to achieve the desired number of dipoles. The ddscat executable obtains its input parameters from the file ddscat.par. This file sets up target shape, polarization, wavelengths, effective radii, and number of dipoles. Setting the target shape parameters accordingly and leaving the lattice separation set at unity in the subroutine reapar.f obtains the desired number of dipoles. The CALLTARGET executable is a user interactive program used to generate targets based on user input of interdipole separation

and target shape. The program produces an ASCII output file, target.out, which must be passed into the ddscat.par file under the target shape option [3]. Both methods to generate dipole arrays are effective because both are based on the same governing principles mentioned in reference [3].

The DDSCAT generates a few output files after the executable files are run for simulations. Two output files, mtable and qtable, are the most important output files. The mtable file contains the dielectric constants that were used during the simulations. [3]. The qtable file contains a list of the scattering cross section values computed by the DDSCAT main routine. These values include  $Q_{ext}$ ,  $Q_{abs}$ ,  $Q_{sca}$ . These values are related and calculated with the following equations.

$$Q_{ext} \equiv Q_{sca} + Q_{abs} \quad (2.5)$$

$$Q_{sca} = \frac{C_{sca}}{a_{eff}^2} \quad (2.6)$$

Other output files can be generated such as binary output files. This can be selected in the input parameter file, ddscat.par, before the simulation is executed.

### 2.2.2 Iterative Solver Algorithms

Within the input file, ddscat.par, the iterative solver is selected. Two iterative solvers are available with the DDSCAT code, the Preconditioned BiConjugate Gradient with Stabilization (PBCGST) and the Complex Conjugate Gradient (PETRKP). The accuracy of the scattering efficiency factor,  $Q_{sca}$ , is dependent upon the accuracy of the solver used. The solvers are computed by the matrix equation  $\mathbf{AP} = \mathbf{E}$ . The iterative solver output can be seen in the file ddscat.log\_000. The output file lists the number of

iterations taken to complete the simulation and the scattering cross section magnitude that was calculated during the simulation. A third column in the output file lists the fractional error calculated during each iteration.

### **2.3 Mie Theory**

Mie theory, also known as Mie scattering, is the main theory the DDSCAT calculations were compared to. Mie theory proposes a solution to Maxwell's equations for spherical particles when the electromagnetic field is scattered by these particles. Mie theory is commonly used to analyze the properties of biological tissues [4]-[6].

For the homogenous target simulations a Mie theory graph of scattering calculations over a common wavelength range was selected for comparison. The graph contains Mie theory calculations for both lossless and lossy spheres.

For the inhomogeneous target, a model of a coated sphere was used. Again different refractive indices were investigated and a range of wavelengths was chosen. The simulations from DDSCAT for the inhomogeneous target were compared to many graphs from reference [4], which are discussed in the Analysis chapter.

### 3. APPROACH AND IMPLEMENTATION

#### 3.1 Iterative Solver Simulations

To ensure that the scattering magnitude of the DDSCAT simulations is accurate, the iterative solvers are analyzed. To evaluate the accuracy of these solvers, an example from Figure 1 of reference [5] is selected with refractive index,  $m=6$  and one point is selected at the highest peak of the graph. Using the ddscat executable, ddscat.par is set up to generate a sphere with an effective radius of  $6.33\mu m$ , one wavelength corresponding to the selected point,  $N=1045$  dipoles, and utilizing the PBCGST solver. The number of dipoles are at a minimum value of the  $f(N)$  function in reference [4]. The dielectric material is set to  $m=6$  in the diel.tab file. Polarization is set for both incident and orthogonal polarization and three orientations are implemented to obtain more accurate results. With an increase in the number of orientations, CPU time increases. Therefore, a small but adequate number of orientations are selected. When the target contains multiple orientations, the target is rotated in the frame to capture different points of the microwave reflection to increase the accuracy of the calculations. Two polarizations and three orientations produced six values of  $Q_{sca}$ , which are averaged and obtained from the output file w00r00kori.avg. The ddscat.log\_000 contains the number of iterations and error per iteration. The PETRKP solver is compared to the PBCGST solver by observing its error over iterations. The fractional error over number of iterations is graphed for six curves to show the accuracy of the  $Q_{sca}$  values obtained by using the PBCGST solver and can be seen in Figure 2a and 2b. In Figure 2 the error curves corresponding to the orientations are separated into Figure 2a and Figure 2b for easier viewing due to the non-

linear behavior of the curves. The same input parameters are used to obtain the accuracy of the PETRKP solver. Six curves are plotted to represent the three orientations and two polarizations; however, only curves 3 and 6 can be observed. In Figure 3, curves 1, 2, 4, 5, and 6 all have similar behavior and overlap each other. The bold line in the legend represents curve 6, the marked lines are beneath curve six, and the dashed line represents curve 3, which corresponds to the second orientation and first polarization. Both solvers presented unique results that are analyzed for the best accuracy.

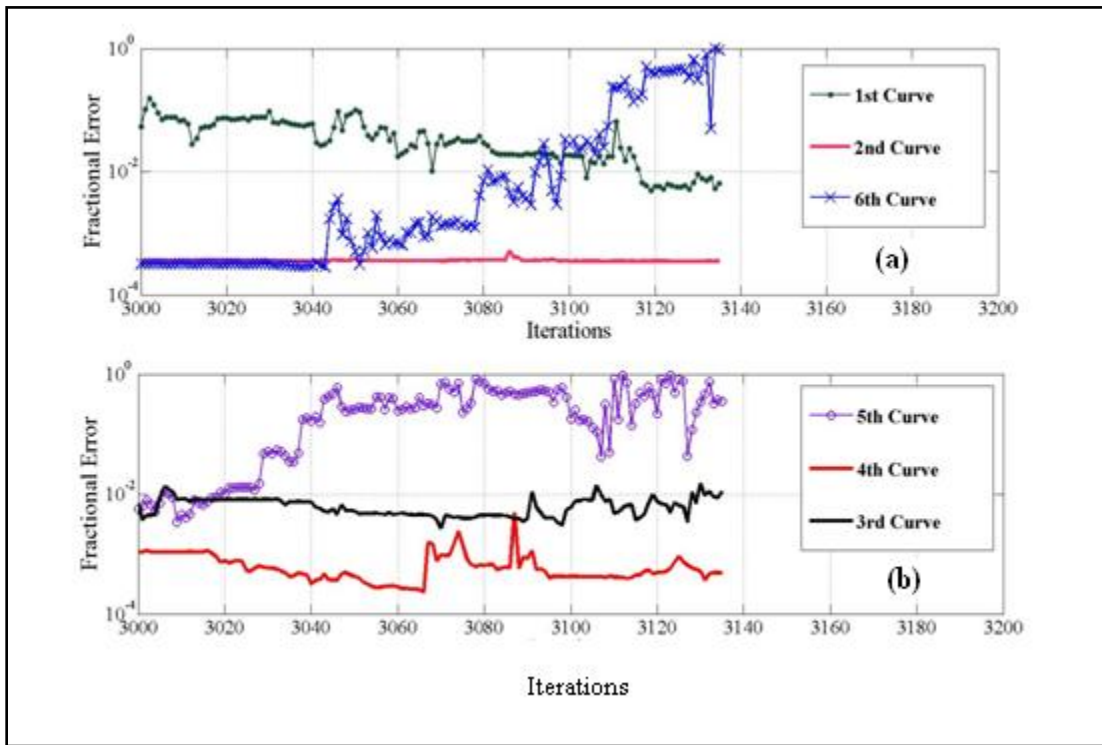


Figure 2. Fractional Error vs. Iterations for PBCGST solver

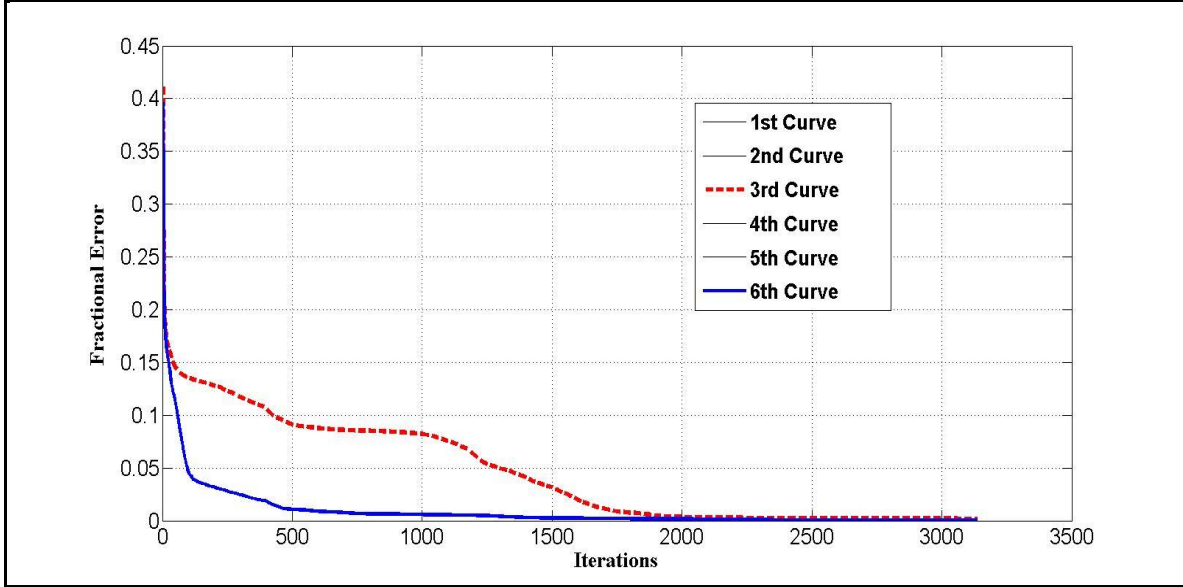


Figure 3. Fractional Error vs. Iterations for PETRKP

### 3.2 Homogeneous Target Simulations

A homogeneous, spherical target is chosen for the simulations because the DDSCAT simulations can be compared to Mie theory calculations. Examples in the DDSCAT user guide are generated to become familiar with the operation of the executable files and input parameter files.

A spherical target is composed of an effective radius equal to  $6.33\mu\text{m}$  and a refractive index of  $m=6.0$ . In the `ddscat.par` file, the spherical shape is selected to be ELLIPS, and the number of dipoles is selected by choosing appropriate, equal values for the shape parameters, PAR1, PAR2, and PAR3. The refractive index,  $m$ , is recorded in the `diel.tab` file and read from `ddscat.par`. Fifty wavelengths are selected from  $.628\mu\text{m}$  to  $6.28\mu\text{m}$  and the effective radius set in the parameter file. Polarization is set to IORTH=2 for both incident and orthogonal polarizations. For this target the orientation is set to zero. Starting with a small number of dipoles, the DDSCAT is simulated four times for

targets differing only in number of dipoles. The scattering cross section magnitude is graphed versus the wavelengths and compared to the Mie theory graph shown in Figure 1b of [5]. The DDSCAT simulation for a losses sphere can be seen in Figure 4.

A lossy spherical target is composed of an affective radius equal to  $6.33 \mu\text{m}$  and a complex refractive index equal to  $m=6+0.01j$ . The shape parameters in `ddscat.par` are set for  $N=2197$  dipoles, and all other parameters are set up identical to the first target that is explained previously. Again the scattering cross-section magnitude is graphed versus the wavelengths. This simulation shown in Figure 5 is compared to the complex Mie theory graph shown in Figure 1c of [5].

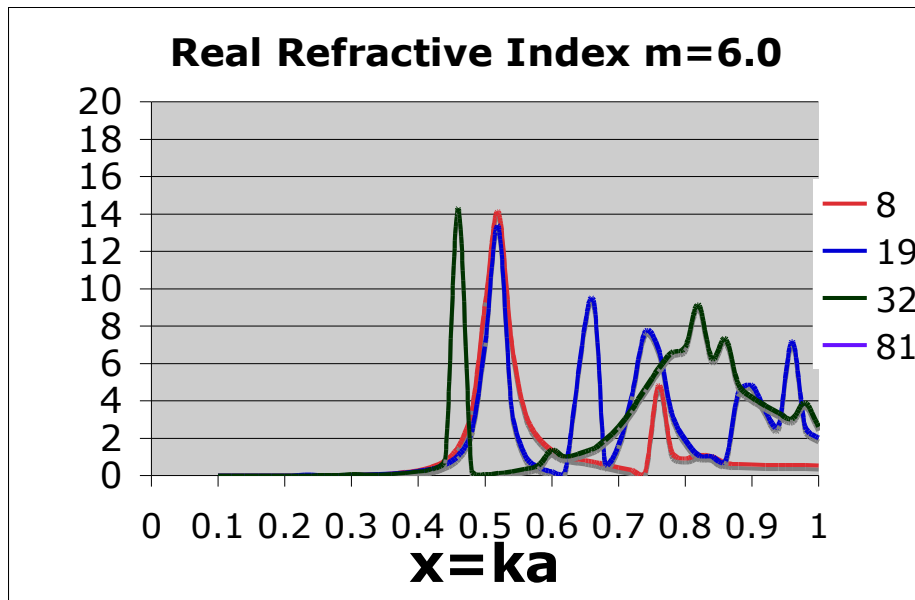


Figure 4. Spherical Homogeneous Target with  $m=6.0$  using 8, 19, 32, and 81 Dipoles.



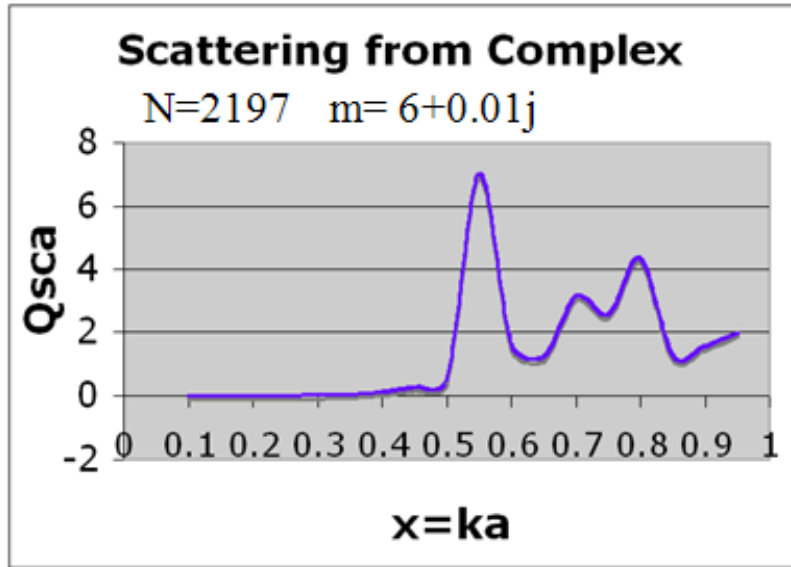


Figure 5. Homogeneous spherical Target with  $m=6+0.01j$  using 2197 Dipoles.

### 3.3 Inhomogeneous Target Simulations

The composition of the female breast is made up of lobes, ducts, and other breast tissues. To model a breast more effectively, a target made up of more than one material must be used. For this reason, an inhomogeneous target made up of simply two materials is studied. Figure 6 shows the structure of the inhomogeneous target. The sphere is composed of two regions and two effective radii. Region 1 forms a small sphere and region 2 acts as a spherical shell to “coat” the small inner sphere.

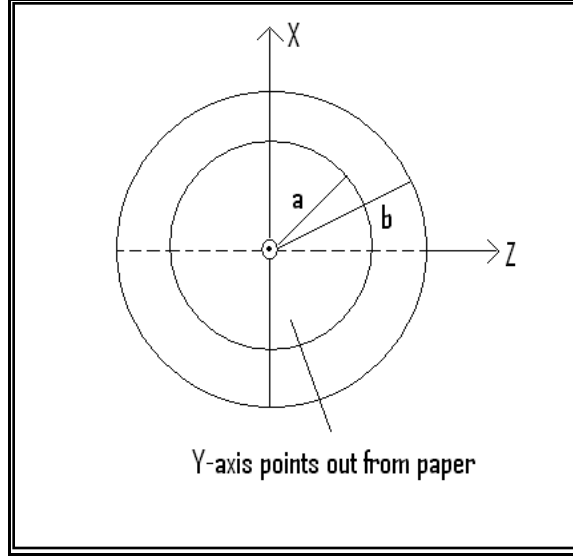


Figure 6. Geometry for scattering of a Inhomogeneous Target [4].

For the inhomogeneous target, basic equations govern the scattering coefficients. These equations relate the affective radius to the frequency for each region of the inhomogeneous sphere. These equations are listed below:

$$q = \frac{\alpha}{v} \quad (3.1)$$

$$\alpha = \frac{2\pi a}{\lambda} \quad (3.2)$$

$$v = \frac{2\pi b}{\lambda} \quad (3.3)$$

For comparison with the inhomogeneous simulations, Figure 5.2 of [6] is selected. The graphs in Figures 5.2 and 5.3 of [6] illustrate the scattering of an inhomogeneous sphere with set ratios of  $\alpha/v$ . The Mie theory graphs show the ratio of  $\alpha/v$  values for small values of  $v$  and large values of  $v$ . For the simulation, the refractive indices are set to

$m_1=2.1050$  and  $m_2=1.4821$ . The parameter  $\nu=1.6$  is selected and appropriate wavelengths for the simulation are calculated from the equations 3.1-3.3 based on this parameter. A simulation is generated using 280 dipoles and the results are seen in Figure 7.

Another figure is selected for further exploration of the inhomogeneous code, and this was Figure 5.5 of [6]. For simulation of the inhomogeneous target, the effective radius for region 1 was set to  $a_{\text{eff}}=1\mu\text{m}$ . The radius for region 2 is calculated appropriately. Simulations are generated for  $N= 81, 552,$  and  $8217$  dipoles. Because the target contains two regions, three shape parameters for each region are listed in `ddscat.par` to generate the desired number of dipoles. The effective radii parameter was set to 2 for the radii  $a$  and  $b$ , and two refractive indices were recorded in `diel.tab`,  $m_1=1.59-.66i$  and  $m_2=1.33$ . The simulation is designed to keep the radius,  $a$ , of region 1 constant while the radius,  $b$ , is increased. To perform this, a certain ratio of  $\alpha/\nu$  is maintained. The DDSCAT simulations are shown in Figure 8 and compared to Figure 5.5 of [6] with  $q=0.2$ . These graphs are discussed in the Analysis of Chapter 4.

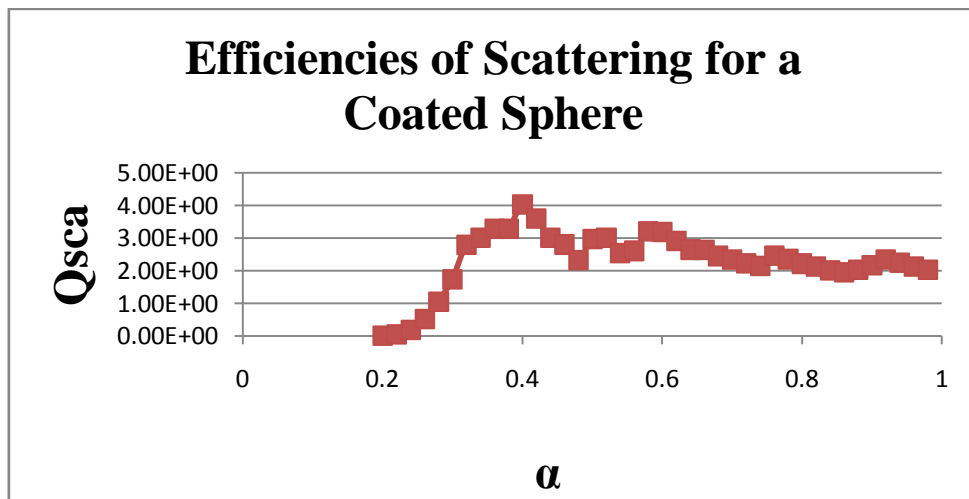


Figure 7. Efficiencies of Scattering for a Coated Sphere for  $\nu=1.6$

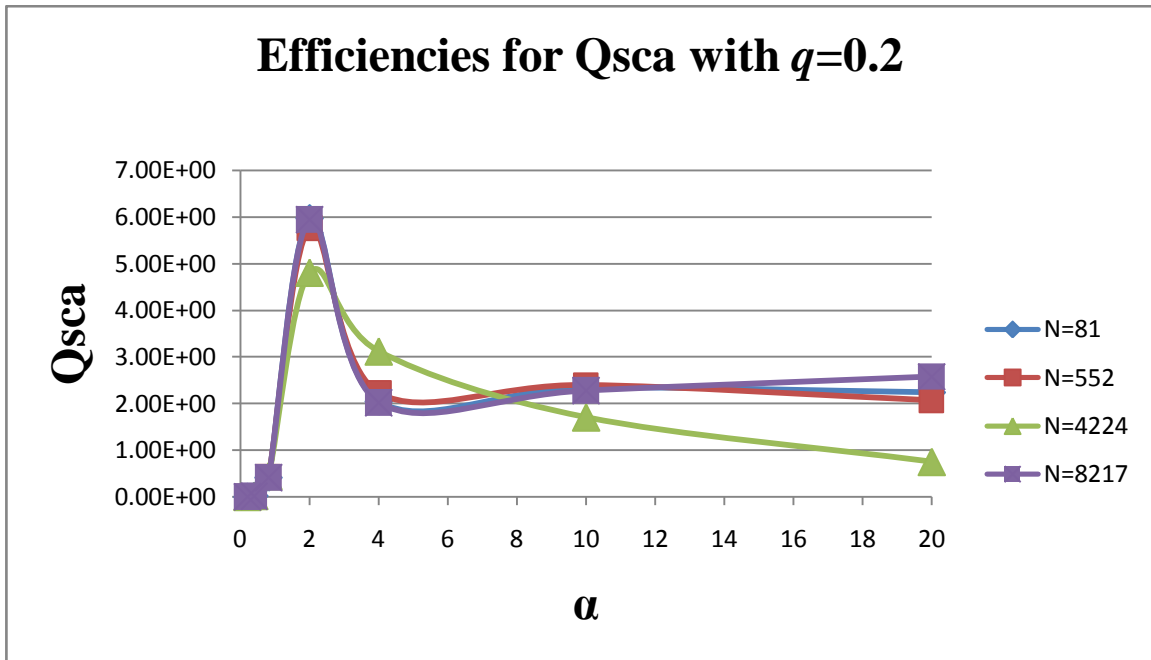


Figure 8. Efficiencies for Scattering with  $q=0.2$

## 4. ANALYSIS

### 4.1 Analysis of Iterative Solvers

The accuracy of the DDSCAT code is analyzed for its potential use to enhance the imaging of breast tumors. The tests performed with the DDSCAT evaluated the accuracy of the scattering efficiency factor based on the iterative solvers and the overall accuracy compared to Mie theory. Two iterative algorithms are compared by plotting the fractional error versus number of iterations. The PBCGST solver shows large fluctuation in error over iterations. Two of the curves contained large error at the last iterations revealing a problem with the  $Q_{sca}$  values. The curves with large fractional error at the final iterations are discarded because the  $Q_{sca}$  values were negative. These negative values have no physical meaning because  $Q_{sca}$  is always positive due to the squared modulus of the scattered field. Using the PETRKP solver obtained the most desired results. The number of iterations versus fractional error is graphed for the PETRKP solver and shows the error decreasing exponentially with increasing iterations. All six curves follow this behavior, and many of the PETRKP curves lay on top of each other. No negative  $Q_{sca}$  values are found when using the PETRKP solver. Because of this and the decreasing error over iterations, the PETRKP solver provides the most accurate  $Q_{sca}$  values. Both solvers have different advantages; however, to obtain precise results using either solver, the calculations of the algorithms must be done with double precision. Currently the DDSCAT is executed with single precision. Although the PETRKP solver requires longer CPU time than the PBCGST, the PETRKP is used when comparing the DDSCAT approximation method with Mie theory due to its accuracy. Further research must be

conducted to increase the precision of the algorithms and explore the accuracy and CPU time with increased number of dipoles and effective radii.

## 4.2 Analysis of Homogeneous Target Simulations

Once the accuracy of the scattering efficiency factor is determined and an appropriate solver is analyzed, the DDSCAT is also tested for overall accuracy. Before producing a graph to compare with the analytical solution, examples from the user manual are explored and reproduced. The examples produced in reference [3] are correctly obtained and compared to Mie theory with small overall error [3]. The knowledge obtained from exploring the user manual examples is applied to produce the example in Figure 4 of reference [5]. The `ddscat.par` file is set up to generate the graph in Figure 1b of reference [5] with a refractive index,  $m=6$ , using the PETRKP iterative algorithm. At first a small amount of dipoles are used to generate the homogeneous spherical target as explained in chapter 3.2. For  $N=8$  and  $N=32$  the behavior of the simulation followed Figure 1 of [5] around  $x=.5$ , however, the latter part of the scattering curve did not match the correct Mie theory behavior. This simulation revealed that more dipoles needed to be used to for the target so it would be accurately represented. The function shown in Eq. 2.3 is used to select an appropriate value of dipoles. The simulation was run again for  $N=1045$  dipoles, but the behavior of the scattering continued to only match the Mie theory graph in Figure 1b of [5] up to  $x=.5$  dipoles. After running successive simulations varying the number of dipoles, full theoretical behavior is not obtained. Another homogeneous target with a lossy refractive index of  $m=6+.01j$  is generated with  $N=2197$  dipoles. This graph, shown in Figure 5 follows the behavior of the Mie theory graph, Figure 1c of [5] up to  $x=0.8$ .

This simulation model is the closest, even though it still contained substantial error. According to reference [4], it was found that the DDSCAT has requires a large amount of dipoles when simulating scattering coefficients for high values of  $m$ . It is for this reason that the simulations in Figures 4 and 5 show large error. The DDSCAT would require a large amount of dipoles for  $m=6$  and  $m=6+.01j$  causing the CPU time for a simulation to increase significantly. Since the CPU time varies as  $N^2$  [4], these simulations are not explored further.

### 4.3 Analysis of Inhomogeneous Target Simulations

The inhomogeneous, spherical target generated is simulated for different dipole values across a spectrum of wavelengths. During the simulations different affective radii for both region 1 and region 2 are used.

At first the graphs in Figures 5.2 and 5.3 of [6] are used as the comparison graphs, however none of the simulations generated for the differing  $\alpha/v$  ratios are accurate or consistent. The most consistent simulation with the theoretical graph can be seen in Figure 7. The graph simulated in Figure 7 has very high error and only slightly follows the behavior of the theoretical curve. Many parameters such as affective radii, number of dipoles, polarization, and orientation are changed to try and produce an accurate simulation. For all of the simulations generated the data is invalid and non-convergent. Because of this, a different graph, Figure 5.5 of [6], is chosen to replicate. This graph focused on one  $q$  value over varying frequency. The DDSCAT simulations can be seen in Figure 8. Even with increasing the number of dipoles, the  $Q_{sca}$  values are similar for every simulation. As seen in Figure 8, the first tall peak of the curves almost matched the

theoretical curve. However, the simulated curves are slightly larger in magnitude and shifted slightly to the right. Also, the behavior of toward the end of the curves does not match the theoretical curves at all. Many methods of changing dipoles, polarizations, and effective radii are used to improve the behavior of the curves. Even with parameters adjusted in the input file, the same output behavior as Figure 8 is obtained.

The reason for this simulation behavior and the erroneous scattering coefficients is unknown. In the case of this inhomogeneous spherical target, the refractive index was set low, so as not to incur high CPU times and unwanted inaccuracy. Further research must be conducted to analyze the algorithms of the DDSCAT which calculate scattering for inhomogeneous targets to tell which parameters need to be adjusted to obtain the desired scattering output.



## 5. CONCLUSION

### 5.1 Summary

The DDSCAT program is analyzed for its iterative solvers and its accuracy in simulating scattering coefficients for spherical targets. A large amount of time is spent on both learning the program by investigating the subroutines which calculated the scattering magnitudes and experimenting with the input parameter file by generating example targets, analyzing the iterative solvers, and studying the homogeneous spherical target.

The iterative solvers are analyzed for multiple iterations and the fractional error is recorded. It was found that the PETRKP solver, although much slower than the PBCGST solver, had better accuracy for the scattering coefficients. However, when large amounts of dipoles are used to generate a target, the CPU time significantly increased because the PETRKP solver was used. This poses a dilemma because for large refractive indices, CPU time is already on the order of  $N^2$ . Also, the solvers are analyzed with single precision and double precision is needed for more accurate conclusions.

Multiple homogeneous and inhomogeneous targets are simulated and analyzed. These targets contained varied refractive indices and are composed of differing amounts of dipoles which are calculated using the  $f(N)$  function.

The homogeneous targets simulated showed accurate scattering values when compared to the Mie theory graphs up until a certain point in the wavelength spectrum. These targets also tended to obtain better accuracy when higher amounts of dipoles are used to compose the targets and when complex refractive indices are used. After analyzing other research concerning the DDSCAT, it is concluded that high values for

refractive indices produced large scattering error if the target is not composed of an adequately large amount of dipoles. It is also concluded that the amount of dipoles needed for the refractive index used would be too large to simulate because of increased CPU time.

The inhomogeneous target simulations are the least accurate of all the simulations. The coated sphere is simulated many times, each time varying an input parameter, such as frequency, radii, or dipoles, in order to increase accuracy. The most accurate simulation is conducted for  $q=0.2$ , but even this simulation varied greatly from the theoretical solution. More extensive research is needed to analyze the algorithms calculating the scattering coefficients for inhomogeneous targets.

From this research, execution of the DDSCAT is learned for two types of targets. The overall accuracy of the DDSCAT calculations for scattering magnitudes remains unsolved for high values of  $m$ . For low values of refractive indices, other references and the DDSCAT user guide, show the DDSCAT to produce low, desirable error. Further research must be performed to test the DDSCAT at these large refractive indices, and more research must be conducted on the simulation of inhomogeneous targets.

## References

[1] Imaginis, “Breast Cancer: Statistics on Incidence, Survival, and Screening”, [Online document] 2008, [2008 August 20], Available at:

<http://www.imaginis.com/breasthealth/statistics.asp>.

[2] BreastCancer.org, “Breast Cancer Statistics”, [Online document] 2009, [2008 November 26] Available at:

[http://www.breastcancer.org/symptoms/understand\\_bc/statistics.jsp](http://www.breastcancer.org/symptoms/understand_bc/statistics.jsp)

[3] Draine, B.T., and Flatau, P.J. 2003, “User Guide for the Discrete Dipole Approximation Code DDSCAT.6.0”, <http://arxiv.org/abs/astro-ph/0309069>

[4] Drain B.T., “The Discrete-Dipole Approximation and Its Application to Interstellar Graphite Grains,” *The Astrophysical Journal*, 333: 848-872, 1988 October 15

[5] Barber. P.W., Owen, J.F, and Chang, R.K., “Resonant Scattering for Characterization of Axisymmetric Dielectric Objects,” *IEEE Transactions on Antennas and Propagation*, Vol. AP-30, No. 2, March 1982

[6] Kerker. M., “Chapter 5: Scattering by Stratified Spheres” in *The Scattering of Light and Other Electromagnetic Radiation* Loebel E.M., New York and London: Academic Press, 1969, pp. 189-254.